IEEE Access
Multidisciplinary | Rapid Review | Open Access Journal

SPECIAL SECTION ON GIGAPIXEL PANORAMIC VIDEO WITH VIRTUAL REALITY

Received August 4, 2020, accepted August 18, 2020, date of publication August 27, 2020, date of current version November 4, 2021.

Digital Object Identifier 10.1109/ACCESS.2020.3019833

Analysis of Earthquake Emergency Command System According to Cloud Computing Methods

CHEN CHENG, WENSHENG CHEN, YANG LI, YAO JI, SHICHUAN NIU, YING HOU, QIQIAN GUO, AND XUCHAO CHAI

The Second Monitoring and Application Center, CEA, Xi'an 710000, China

Corresponding author: Wensheng Chen (chenwensheng@smac.ac.cn)

ABSTRACT An earthquake emergency command system is designed based on cloud computing and the Internet of Things (IoT) to mitigate slow information acquisition, low processing efficiency, and weak information storage and communication ability in earthquake rescue. First, cloud computing technology is introduced, and a traditional earthquake emergency command system is analyzed comprehensively. Then, the characteristics of midwave infrared remote sensing data are explored before and after recent earthquakes in China based on satellite remote sensing data. Subsequently, a new earthquake emergency command system is built based on cloud computing and IoT technology along with data from satellite midwave infrared remote sensing. Finally, system feasibility is evaluated. The results show that surface radiation changes significantly before an earthquake; infrared brightness and temperature fluctuates drastically; and the abnormal region gradually approaches the epicenter of the earthquake. The peak value of the relative power spectrum in the earthquake is more than 9 times the average. In conclusion, the proposed emergency command system based on satellite remote sensing data, cloud computing, and IoT can yield good evaluation results (5.36), demonstrating that multidimensional satellite thermal infrared remote sensing data analysis can improve the accuracy of earthquake prediction. The proposed earthquake emergency command system based on satellite remote sensing data combined with cloud computing and IoT technology can also provide a basis for optimizing earthquake rescue strategies.

INDEX TERMS Cloud computing, Internet of Things, earthquake emergency command system, satellite remote sensing data, relative power spectrum, brightness temperature difference value.

I. INTRODUCTION

Earthquakes are a natural disaster that can produce severe destruction. Earthquakes are caused by plate activity and typically occur at the junction of various plates [1]. There are seven earthquake zones in China. Certain plates in the earthquake zone are not active, while others are active. Earthquakes occur frequently in areas located within earthquake zones and along their peripheries [2]. Reports show that 8 violent earthquakes of magnitude eight or above have occurred worldwide since 2000. The death tolls in earthquake regions tend to be high, yielding high economic losses, permanent destruction and pain to people living in earthquake regions [3]. In China's ''5.12'' violent earthquake in 2008, 69,227 people were killed, 17,923 people were missing, 374,643 people were injured, and the economic loss was above RMB 1 trillion [4]. Currently, the ability to predict earthquakes is not adequate. Although technology has developed rapidly since 2000, research in earthquake prediction has been slow. With the rapid development of satellite remote sensing technology, infrared data have also been used in earthquake research, and satellite infrared remote sensing data have also yielded achievements in earthquake research [5]. In recent years, progress has been made using satellite thermal infrared data to study earthquakes, and quantified spatiotemporal evolution feature information has also been obtained, which is important to track and characterize thermal anomalies related to earthquakes with these data to provide a basis for the accurate prediction of earthquakes.

Apart from predicting earthquakes in advance to reduce damage, communication of information relevant to surviving earthquakes can also markedly help to reduce losses in earthquake regions. As an important tool in earthquake emergencies, earthquake emergency command systems are

The associate editor coordinating the review of this manuscript and approving it for publication was Zhihan Lv.

valuable. During the period of the 13th 5-year plan, the Chinese government constructed an earthquake relief headquarters system in every province that covers every county [6]. However, there are gaps due to different development levels in various areas in China. Due to improper communication, it is impossible to describe the exchange of information among multiple departments and multiple areas, and conduct rescues when violent earthquakes occur. It is also difficult to create a site where various departments respond to earthquakes coordinately [7]–[9]. Therefore, developing a method that can improve information resource integration and communication among different levels and various departments during earthquake emergencies is critical. The emergence of cloud computing and IoT technology has improved information sharing, mass data storage, and data mining. The application of cloud computing and IoT technology to emergency decision information systems can improve information shared for emergency decisions. Thus, management during earthquake processing is improved, rescue efficiency in earthquakes is improved, and more rescues can be achieved.

Cloud computing and IoT technology are used to develop an earthquake emergency command system to address various problems in earthquake emergency rescue commands. First, cloud computing and IoT technology are introduced, and the requirements, feasibility, and process of the system are analyzed. Then, the spatiotemporal characteristics of thermal anomalies of certain earthquakes in China in recent years are explored using satellite infrared remote sensing data. Combining satellite infrared remote sensing data with cloud computing and IoT technology, the structure and functions of the earthquake emergency command system are designed. Finally, indices are developed for feasibility analysis. This study provides results that can improve earthquake rescues in China

II. LITERATURE REVIEW

A. EARTHQUAKE EMERGENCY COMMAND RESEARCH

The occurrence of earthquakes affects the production of society, people's lives and other aspects, and can evolve into a social crisis [10]. Therefore, emergency response to earthquakes and their management has become an important research topic of today's social management and is important to the harmonious development of the economy and society. Earthquake emergency commands are the core system of earthquake emergency management, which coordinate all aspects of earthquake rescue operations and promote the effectiveness of rescue operations [11], [12]. Currently, many organizations, experts, and scholars have tried to construct an earthquake emergency command system with various components, including emergency command systems, models, systems, and system evaluations. Wang *et al.* (2019) showed that an earthquake can have a strong impact on the operation of schools and proposed a university earthquake emergency system based on multivariate data monitoring, in which decision-making methods include the analytic hierarchy process (AHP), linear regression method, earthquake disaster simulation, and expert assessment. The authors found that the system can respond more quickly and reasonably to earthquakes than existing systems [13]. Xu *et al.* (2020) proposed a mapping method that uses template matching to quickly make earthquake emergency maps. This method can update the template after an earthquake using information from an earthquake model to automatically draw an emergency map. The reliability of this method was verified by a case study [14]. Ahmadzadeh *et al.* (2019) evaluated the performance of earthquake stress command headquarters at Alborz Medical Sciences University for earthquakes and disaster risk management, and found that command headquarters responded in a timely manner and could make effective decisions [15]. To date, there have been many studies of earthquake emergency systems; however, most focus on disaster management after an earthquake.

B. RESEARCH STATUS OF CLOUD COMPUTING TECHNOLOGY

Cloud computing is a distributed computing method that primarily refers to the process of computing and decomposing massive data into many small programs through the network ''cloud''. Then, a system composed of multiple servers will analyze and process these small programs and finally return the processing results to users [16], [17]. Cloud computing is also being used to build emergency systems. d 'Oro *et al.* (2019) built a novel architecture based on cloud computing and IoT technology to improve response capacity, bandwidth demand, privacy, and availability in emergency systems. After verification, the system's structure provided high security and reliability [18]. Facchinetti *et al.* (2019) proposed a software system for indoor emergency response management based on mobile clouds, which can provide people with escape routes and other help in the event of disasters. The software system also markedly improved the reliability and safety of indoor workplaces, and provided information to prepare for and manage various emergencies or events [19]. Ujjwal *et al.* (2019) found that in the event of earthquakes and other disasters, cloud computing and IoT technology can be used to more effectively construct natural disaster prediction models and management systems [20]. Thus, cloud computing has been widely used in disaster prediction and emergency management; however, whether an earthquake emergency command system that includes earthquake prediction based on the cloud computing framework combined with IoT technology must be investigated in more detail.

C. APPLICATION OF SATELLITE REMOTE SENSING DATA IN EARTHQUAKE RESEARCH

There have been many studies of the application of satellite remote sensing data in earthquake research; however, results have not yet described practical applications of this data in real scenarios. Thermal infrared data have potential for use in earthquake space observations. Liu *et al.* (2020) used the

wavelet transform and relative power spectrum to analyze the thermal infrared anomalies of ground earthquakes from MODIS data and then analyzed the correlation between the area coverage and earthquake amplitude. They showed that weak earthquake thermal infrared anomalies can be used to predict earthquakes [21]. Barkat *et al.* (2018) showed that the increase in the Earth's surface temperature is closely related to the earthquake. Calculating the increase in the Earth's surface temperature using the thermal infrared image of the satellite could obtain precursor information of an earthquake [22]. Wei *et al.* (2020) used the time-frequency, wavelet transform, and relative power spectrum methods to analyze the periodic variation of satellite characteristic data, including thermal radiation anomalies, thermal radiation background anomalies, and brightness temperature values [23]. Jing *et al.* (2020) analyzed anomalous microwave brightness temperatures during a strong earthquake in Sichuan Province, China, using the subsection threshold method. They then obtained the anomalous index of the microwave radiation, which indicated that the anomalous microwave brightness temperature was present for 2 months prior to the earthquake [24].

It is critical that earthquake emergency command systems can allow correct decisions to be made by different organizations or persons in the event of an earthquake. Also, research on emergency systems based on cloud computing and IoT technology can improve the efficiency and safety of emergency management systems. Earthquake prediction based on satellite remote sensing data can also improve the reliability of earthquake emergency system decisions. However, currently, earthquake emergency systems based on cloud computing technology are still underdeveloped, and the importance of each system element has not been explored. Therefore, satellite remote sensing data have been used to analyze the thermal infrared anomaly information of certain earthquakes in China in recent years, and IoT technology has been used in earthquake emergency command systems. In this study, an earthquake emergency command system is built based on cloud computing and IoT technology, and the implementation feasibility of this system is evaluated qualitatively and quantitatively. The results of this study are intended to provide a theoretical basis for constructing an effective earthquake emergency command system and improving the efficiency of earthquake rescue operations.

III. METHODOLOGY

A. OVERVIEW OF RELEVANT TECHNOLOGIES

Computing technology is a type of information technology that has been developed in recent years. Through the Internet, computing technology can provide computing resources, including networks, computing storage, data and applications, and perform computational tasks for users in frameworks, platforms or software without users buying various complex hardware equipment and software. Cloud computing features virtualization, on-demand service, high reliability, and dynamic customization, [25] and can be understood as a computing mode extended by parallel and distributed computing or network computing. Cloud computing can breakdown massive computing ability of the network into multiple subroutines, distribute them to multiple servers that compute and analyze data, and feed results back to users. This system can solve various computing issues, including computing ability, storage ability, and load capacity for users, and help users share resources and information [26]–[28].

There are three cloud computing service types: infrastructure as a service, platform as a service, and software as a service. The specific structure of each of these types is shown in Fig. 1. Among the three service types, the application of cloud computing in earthquake emergency management is primarily infrastructure as a service, which must achieve the exchange, update and gathering of information through virtual infrastructure and process various applications coordinately to describe resource integration at the level of information processing [29].

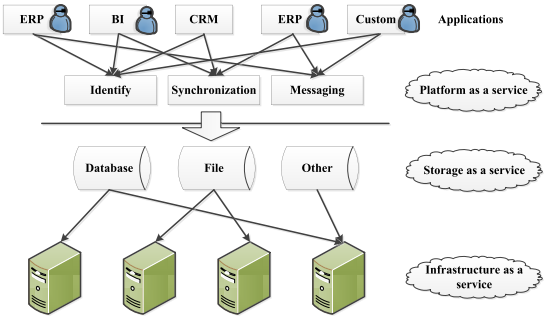

FIGURE 1. Basic architecture of cloud computing.

B. ANALYSIS OF AN EARTHQUAKE EMERGENCY COMMAND SYSTEM BASED ON CLOUD COMPUTING AND IoT

In an earthquake emergency command system based on cloud computing and the IoT, requirements can be divided into two levels: user and functional. Fig. 2 shows the business process diagram of the proposed earthquake emergency command system. The procedure of the whole event is implemented in three stages: before, during, and after. The stage before the event includes prediction, early warning, and information

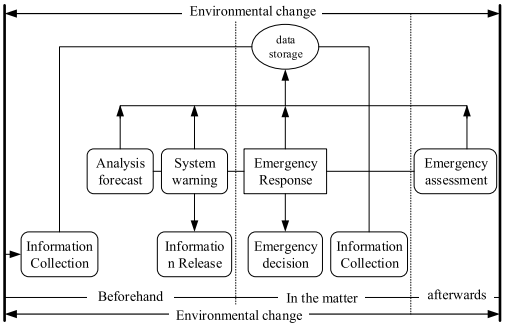

FIGURE 2. Business process diagram of the earthquake emergency command system.

distribution. The stage during the event includes emergency decisions and resource allocation. The stage after the event includes emergency assessment and disaster recovery and reconstruction [30].

Fig. 3 shows the decision diagram of the traditional earthquake emergency command system, and Fig. 4 shows the decision diagram of the earthquake emergency command system based on cloud computing and IoT. Fig. 3 shows that if the earthquake parameter inputs are matched, the system can provide a similar earthquake rescue solution based on existing information. If there is no matching case, the system is invalid, or the solution must be improved or changed, which will require considerable time and labor. The earthquake emergency command system based on cloud computing and IoT can provide real-time data on site. Even if there is no matching solution, the emergency decision can adjust the decision solution [31].

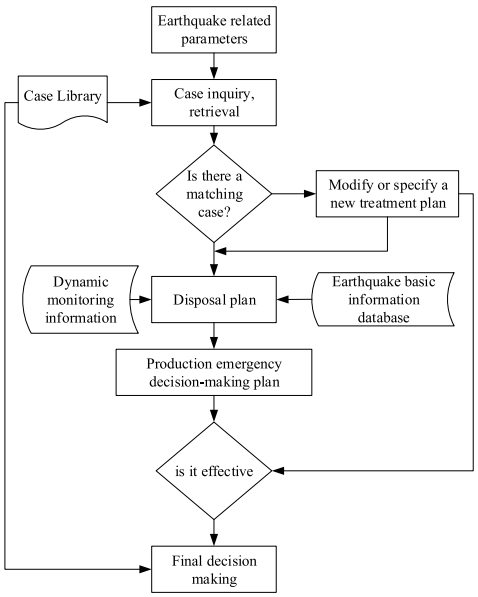

FIGURE 3. Decision diagram of the traditional earthquake emergency command system.

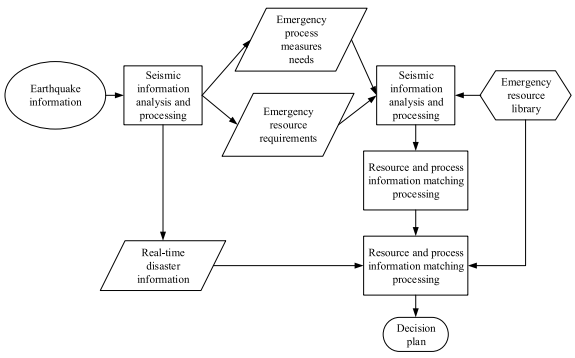

FIGURE 4. Decision diagram of the earthquake emergency command system based on cloud computing and IoT.

C. EARTHQUAKE SATELLITE REMOTE SENSING DATA ANALYSIS BASED ON WAVELET DECOMPOSITION

When satellite remote sensing data are used for earthquake prediction, it is critical to inversely describe abrupt changes in physical parameters, such as temperature, to identify abrupt changes in bright temperatures during earthquakes and then extract infrared heating anomaly practices. The Lipschitz index [32] is used to express the local singularity of the signal.

It is assumed that n is an integer that is not negative, and $n < a \leq n + 1$. If there are two constants A and h_0 (>0) and n degree polynomial *Pn(h),* any $h \leq h_0$, then the equation below is obtained.

$$|f(x_0 + h) - P_n(h)| \leq A|h|^0 \tag{1}$$

In these equations, $f(x)$ is Lipschitz α at point x_0. If $x_0 \in (a, b)$ and $x_0 + h \in (a, b)$, then $f(x)$ is Lipschitz α in the range (a, b).

When a wavelet is used to analyze the local singularity of the signal, the wavelet coefficient depends on the characteristics of $f(x)$ in the x_0 domain and the scale of the wavelet transform. In the wavelet transform, if the function $f(x)$ can be represented by $W_f(s, x)$ and the scale can be represented by S, then the equation below can be obtained.

$$\left|W_f(s, x)\right| \leq K_S^{\alpha} \tag{2}$$

In equation (2), α is the singularity exponent of x_0, and K is a constant. If $\forall x \in \delta x_0$, then the equation below is obtained.

$$\left|W_f(s, x)\right| \leq \left|W_f(x, x_0)\right| \tag{3}$$

In these equation, x_0 is the local extremum of the wavelet transform at scale S. The signal breaks at the maximum of the wavelet transform; thus, it is necessary to determine an optimal transformation scale.

The equation of wavelet transform is as follows.

$$\psi_{a,b}(t) = \frac{1}{\sqrt{a}}\psi\left(\frac{t-b}{a}\right) \tag{4}$$

In equation (4), a and b are constants; $\psi_{a,b}(t)$ is obtained by scaling and translation transformation of the function $\psi(t)$; a is the scaling factor; and b is the translation factor. Given a square-integrable signal a $X(t)$, the equation below is obtained.

$$WT_X(a, b) = \frac{1}{\sqrt{a}}\int X(t)\psi^*\left(\frac{t-b}{a}\right)dt \tag{5}$$

Then, the earthquake signals are processed based on multilevel 1D wavelet decomposition. The signal decomposition method is shown in Fig. 5. After the signal is obtained, it is decomposed into a high-pass signal and a low-pass signal. The low-pass signal refers to part A, and the high-pass signal refers to part D. Then, the two parts are further decomposed separately through a process called wavelet packet decomposition. If the signal is decomposed in N layers, the number of decomposed signals obtained in the N^{th} layer is 2^N, and their bandwidths are adjacent from low to high. The signal of a certain layer can be processed, and the original signal can then

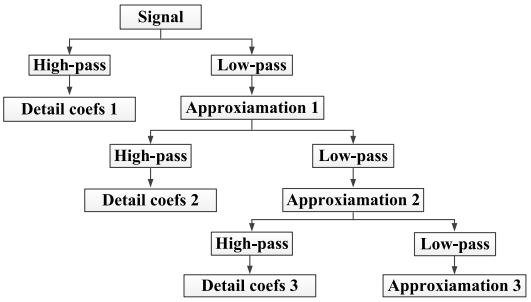

FIGURE 5. Schematic diagram of multiscale wavelet decomposition.

be reconstructed with the retained wavelet packet decomposition coefficients. The coefficients decomposed with the signal wavelet packet decomposition can completely reconstruct the original signal, and the error is small. Compared to the original signal, the reconstructed signal retains the low-frequency part and excludes the high-frequency part; thus, the signal becomes smoother. The detail coefficient 3 describes the highest frequency band of the signal, which represents the finest detail of the signal.

The midwave infrared data product of China's static weather satellite FY-2C/E/G is used in this study. The effective detection range of the satellite is 45°∼165°E, 60°S∼60°N, and is observed every 1 h or 30 min for 24 h per day. The file can be downloaded from http://satellite.cma.gov.cn/. In this study, the observation files are obtained from 23:00 to 4:00 Beijing time to avoid direct solar radiation. The converted data are middle wave infrared brightness temperature data, including 5°∼50°N, 55°∼150°E. Data are stored in binary format, and the database is built on a yearly basis. Multiscale wavelet decomposition is used to decompose earthquake infrared satellite data, and then the abnormal changes in surface radiation before and after the earthquake are analyzed.

D. SURFACE BRIGHTNESS TEMPERATURE VALUE ANALYSIS BASED ON SATELLITE INFRARED REMOTE SENSING RADIATION

Satellite remote sensing collects and records ground object thermal radiation information by satellite or airborne sensors, and identifies ground objects and inversion surface parameters using thermal radiation information. In the analysis, the ''blackbody'' radiation law must be considered. In this study, the surface brightness temperature value is calculated based on the Planck radiation law.

$$M_c(T) = \frac{2\pi hc^2}{\lambda^5} \cdot \frac{1}{e^{\frac{hc}{\lambda kT}-1}} \tag{6}$$

In equation (6), M is the radiation function of the black body; T is the absolute temperature (K); λ is the wavelength; h is Planck's constant (6.626 × 10.34 J·s); c is the speed of light (3 × 10.8 m/s); and k is the Boltzmann constant (1.38 × 10.23 J/K). Then, the Planck radiation equation is as follows.

$$B_c(T) = \frac{2hc^2}{\lambda^5\left(e^{\frac{hc}{\lambda kT}-1}\right)} \tag{7}$$

If frequency f is used, it can be expressed as follows.

$$B_f(T) = \frac{2hf^3}{c^2\left(e^{\frac{hc}{\lambda kT}-1}\right)} \tag{8}$$

In this study, the numerical conversion of the satellite instrument is first performed.

$$E_i = A_i \times I_i + B_i \tag{9}$$

In equation (9), i is the channel number; A_i and B_i are calibration coefficients; and I_i is the counting value.

The brightness temperature corresponding to a specific gray value is calculated using the gray-temperature table. Then, the brightness temperature value calculated using Planck's formula is as follows.

$$T_B = \frac{1.438833v}{\ln\left(1 + \frac{1.1910659\times10^{-5}v^3}{E}\right)} \tag{10}$$

In equation (10) above, T_B is the brightness temperature, E is the emissivity after calibration, and v is the central wavelength (cm-1).

Affected by the curvature of the Earth and atmospheric depletion, the detection data of the infrared channel vary with the different zenith angles of the observation points: the closer one gets to the edge of the scan line, the longer the detection path, the more severe the atmospheric depletion, and the smaller the detection value. The final image is darker than the original, which indicates that the adjacent edge darkens. To ensure the authenticity of the collected image, it is necessary to modify it.

$$T = T_B + \Delta T \tag{11}$$

In this equation, ΔT is the correction of temperature. ΔT, and the observation points can be calculated by satellite zenith angle θ.

$$\begin{cases} T = \left(e^{0.00012\cdot\theta^2} - 1\right) \cdot (0.1072 \cdot T_B - 26.81) \\ \theta = \sin^{-1}\left(\dfrac{R_E + H}{R_E}\sin\sigma\right) \end{cases} \tag{12}$$

In equation (12), R_E is the radius of the Earth, H is the altitude of the satellite, and σ is the zenith angle of the satellite (which can be obtained by the detection sequence number of the observation point).

E. ESTIMATION OF POWER SPECTRUM BASED ON MIDDLE WAVE INFRARED BRIGHTNESS TEMPERATURE WAVEFORM

Power spectrum estimation is an important part of data signal processing and can describe the energy distribution of

component power in each frequency of a random signal. In this study, the time domain middle wave infrared brightness temperature data processed by wavelet decomposition are used for Fourier transform with 64 days as the window length and 1 day as the sliding window length to obtain time-frequency spatial data. Then, all frequency power spectrum amplitudes in each pixel are processed based on the average power spectrum amplitude. The calculated relative power spectrum amplitude is considered to be the abnormal multiple. Image processing technology is used to scan the whole space-time and all frequency bands of the relative power spectrum, and the frequency with a large change in the relative power spectrum amplitude is considered to be the dominant frequency and the corresponding period as the characteristic period. When the relative power spectrum value of the abnormal area corresponding to the dominant frequency is above 6 times, the time of the abnormal area lasts above 30 days. The abnormal area is located at the epicenter or the edge of the earthquake area, the distribution of the abnormal area is related to the direction of the fault, and the time of the occurrence of the abnormal area is related to the time of the earthquake. In this case, the data point can be judged as an earthquake anomaly.

In the database built based on the data collected by fy-2c/E/G, China's static weather satellite, all data are binary. The stored pixel is $0.05^\circ \times 0.05^\circ$; thus, the $0.5^\circ \times 0.5^\circ$ region contains a total of 121/d values, and the daily value in this region is the average value of these data. Therefore, the calculation expression of the relative power spectrum in the region of $0.5^\circ \times 0.5^\circ$ is as follows.

$$\bar{w}_i = \frac{\sum_{n=1}^{n=121} w_{in}}{N} \tag{13}$$

where w_{in} is the relative power spectrum value of the nth pixel of the id in the region; $N = 121$; $1 \le i \le 365$.

Then, the background value of the relative power spectrum is expressed as follows.

$$\bar{A}_i = \frac{\sum_{k=1}^{k=10} \sum_{n=1}^{n=121} w_{ink}}{N} \tag{14}$$

In equation (14), w_{ink} is the relative power spectrum value of the nth pixel of the kth year id in the region; $N = 1210$; $1 \le i \le 365$.

Then, the equation for calculating the standard deviation of the power spectrum is as follows.

$$B_i = \frac{\sqrt{\sum_{k=1}^{k=10} \sum_{n=1}^{n=121} \left(w_{ink} - \bar{A}_i\right)}}{N} \tag{15}$$

In equation (15) above, $\bar{A}_i$ is the background value of the relative power spectrum; $N = 1210$; $1 \le i \le 365$.

F. DESIGN OF THE EARTHQUAKE EMERGENCY COMMAND SYSTEM BASED ON CLOUD COMPUTING AND IoT

The proposed system is designed with six layers: physical, transmission, virtual, service seal, system application, and user. The specific system structure is shown in Fig. 6. The physical layer includes hardware, such as computer equipment, network equipment, IoT sensing equipment, site monitoring and data acquisition end, server, and storage equipment, and software. The transmission layer provides the communication network combined with 3D wireless technology and optical fibers. The virtual layer virtualizes the information required by emergency commands, such as the data based on GIS (e.g., the relative power spectrum and the difference in brightness temperature in satellite infrared remote sensing data based on wavelet decomposition analysis) and monitored data (e.g., video information), to conduct classified management and constructs a virtual pool to describe computing, storage, resource gathering and sharing. The service seal layer is the processing layer that transfers the resources of the virtual layer to concrete prediction analysis and decision assistance. The system application layer converts the information format through a service-oriented architecture and processes various information businesses in order. The user layer connects various emergency parts through standardized service access and invocation interfaces [33].

The earthquake emergency command system based on cloud computing and IoT is designed with the functions of information management; prediction and early warning; decision assistance; emergency guarantee; command and dispatch; and simulations. The information management function is used to backup, forward and process earthquake data, as shown in Fig. 7. The information management application architecture combines virtualization of cloud computing to construct a storage system with different stratifications, as shown in Fig. 8.

IV. RESULTS AND DISCUSSION

A. WAVELET ANALYSIS RESULTS OF SATELLITE REMOTE SENSING DATA

On August 25, 2008, the Zhongba earthquake occurred in Zhongba of the Tibet Autonomous Region with epicenters at 31.0°N and 83.6°E, and a magnitude of 6.8. First, the observation data describing the thermal infrared brightness temperature in the area where no earthquake occurred during this time period are considered to be a normal control to comparatively analyze the earthquake data in Zhongba, Tibet. The observation time is from January 1, 2008, to December 1, 2008.

The thermal infrared satellite observation data of 28.4°N latitude and 102.1°E longitude in Sichuan and the date at 29.5°N latitude and 82.7°E longitude when no earthquake occurred on August 25, 2008 in Zhongba, Tibet Autonomous Region within a year are considered for comparison. Fig. 9(a) shows that although there are small-amplitude

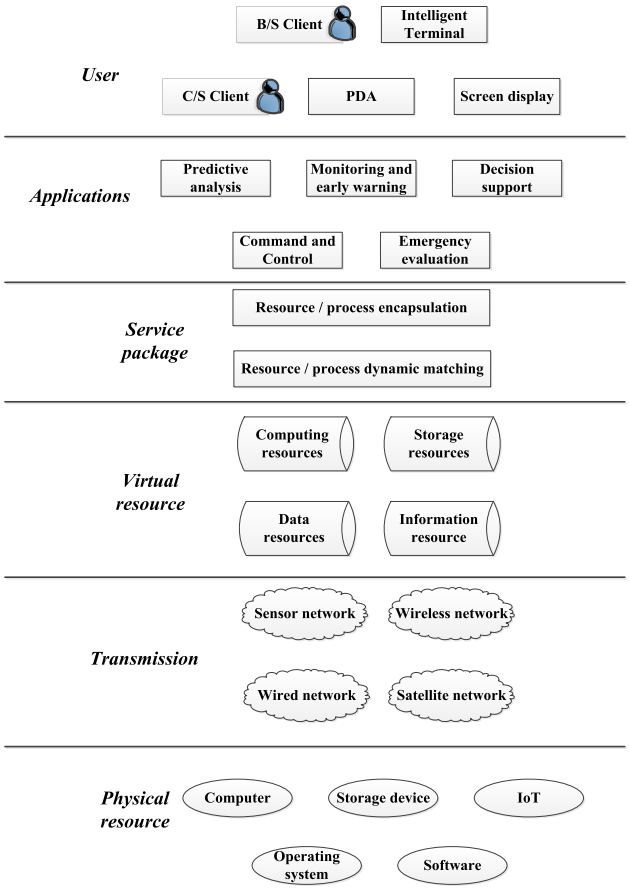

FIGURE 6. Basic structure of the earthquake emergency command system.

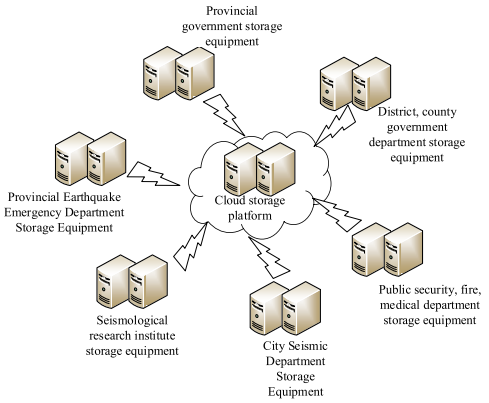

FIGURE 7. Structure diagram of the information management system of the earthquake emergency command system based on cloud computing and IoT.

sudden changes in high-frequency components in areas where earthquakes have not occurred in Sichuan, the overall distribution is relatively uniform. Fig. 9(b) suggests that the low-frequency component (bright temperature in the thermal infrared satellite data) in the area without an earthquake is similar to a sine curve with noise; however, the overall change exhibits some trends. Then, the low-frequency component is

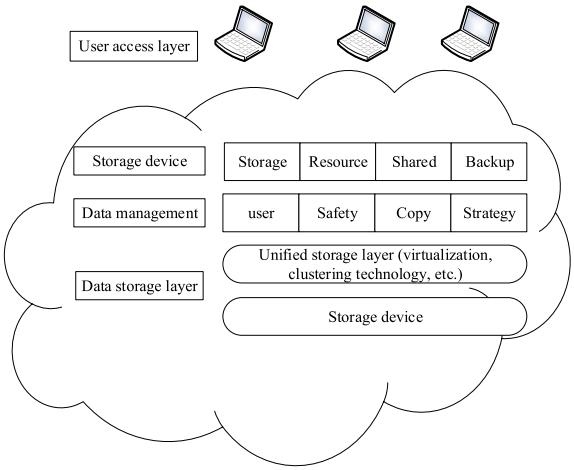

FIGURE 8. Architecture diagram of the information management application of the earthquake emergency command system based on cloud computing and Io.

decomposed by the wavelet. Fig. 9(c) shows that the trend of the low-frequency component (thermal infrared brightness temperature) in this area is similar to a sinusoidal signal with an marked periodicity, which is consistent with the annual change in the surface temperature.

Fig. 9(d) suggests that before the earthquake (May-August 2008) in the Zhongba area of Tibet, there was a trend of abnormally rising high-frequency component signals. Fig. 9(e) indicates that before the earthquake (approximately August 2008) in the Zhongba area of Tibet, there was a marked sudden change in the low-frequency component signal. Then, the low-frequency component is decomposed by the wavelet. Fig. 9(f) shows that the low-frequency component (thermal infrared brightness temperature) exhibited an marked upward trend from June 2008 to August 2008 and then quickly decreased, which indicates that the surface radiation in Zhongba, Tibet, abnormally changed before the earthquake.

B. ANALYSIS ON DIFFERENCE IN SATELLITE THERMAL INFRARED BRIGHTNESS AND TEMPERATURE BEFORE AND AFTER THE EARTHQUAKE

Data from different earthquakes obtained by satellite monitoring are compared for analysis of the thermal infrared temperature difference. The earthquakes include the Ms8.0 earthquake occurred in Wenchuan of Sichuan on May 12, 2008 (epicenter of 31°N and 103.4°E, focal depth of 33 km), Ms6.8 earthquake occurred on August 25, 2008 in Zhongba of Tibet (epicenter of 31°N and 83.6°E, focal depth of 10 km), Ms6.6 earthquake occurred in Jinghe of Xinjiang on August 9, 2017 (epicenter of 44.27°N and 82.89°E, focal depth of 11 km), and Ms5.7 earthquake occurred in Songyuan of Jilin Province on May 28, 2018 (epicenter of 45.27°N and 124.71°E, focal depth of 13 km). Fig. 10 (b), (c), (d), and (e) show that the satellite thermal infrared changed from weak to strong before the each earthquake and rapidly decreased after

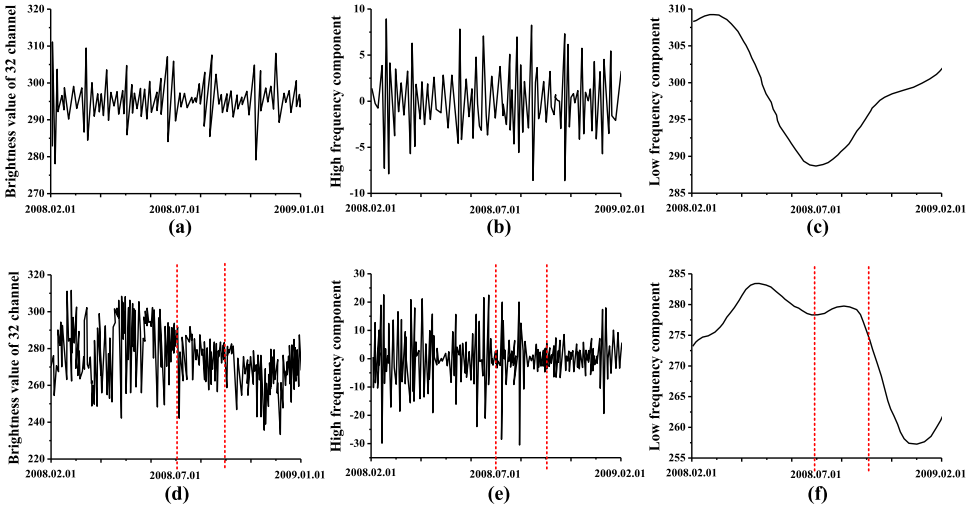

FIGURE 9. Variation of thermal radiation and results of wavelet decomposition from January 1, 2008, to December 1, 2008, in regions with no earthquake in Sichuan and Zhongba, Tibet. Note: Figs. (a), (b), and (c) show changes in the high-frequency component signal, changes in the low-frequency component signal, and wavelet decomposition of the low-frequency component signal in the area without earthquakes, respectively. Figs. (d), (e), and (f) show changes in the high-frequency component signal, changes in the low-frequency component signal, and wavelet decomposition of the low-frequency component signal in the area with earthquakes, respectively.

each earthquake within 1 year in Sichuan Province, Tibet, Xinjiang Province and Jilin Province. However, the brightness temperature difference curve shown in Fig. 11(a) in the period without earthquakes remains relatively constant.

C. ANALYSIS OF INFRARED ANOMALIES IN EARTHQUAKE MIDDLE WAVES

First, the earthquake area is scanned for half a year. Fig. 11(a), (b), (c), and (d) show that the relative power spectrum can describe the infrared anomalies in earthquake waves. In the first month before an earthquake, an abnormal area gradually appears and approaches the epicenter as time continues. The area then reaches the maximum temperature in the month of the earthquake and then gradually decreases after the earthquake.

Then, a time series analysis of the relative power spectrum in the region of $0.5° \times 0.5°$ near the epicenter of each region is performed. Fig. 12(a), (b), (c), and (d) show that there are marked abnormal changes in the time series curve of each region within one year of each earthquake. Additionally, the abnormal values reach their peak within one week of the earthquake, which are 8 to 16 times the average values. The time of the average amplitude above 2 times the average lasts for approximately 30 days. Concurrently, the difference with which the regional time series curve deviates from the background value and that of the standard deviation time series curve increase, particularly the peak of the power spectrum deviating the most during the earthquake.

Table 1 shows that peak temperatures are typically above 9 times the average temperature in each region in the relative power spectrum of the infrared middle wave in the earthquake. Peaks also tend to occur more often before the earthquake, with an average duration greater than twice within 30d∼70d.

TABLE 1. Analysis of abnormal characteristics of the middle wave infrared relative power spectrum in earthquakes.

Place	Time	Magnitude	Peak multiples	Time of the peak	Duration greater than 2 times
Wenchuan, Sichuan	2008.05.12	8.0	13	4d after earthquake	55d
Zhongba, Tibet	2008.08.25	6.8	16	8d before earthquake	68d
JInghe, Xinjiang	2017.08.09	6.6	12	11d before earthquake	51d
Songyuan, Jilin	2018.05.28	5.7	9	8d before earthquake	35d

D. OUTPUT DESIGN OF EARTHQUAKE EMERGENCY COMMAND SYSTEM

Based on the needs of users and the various functions in the system modules, the output interface of the system in

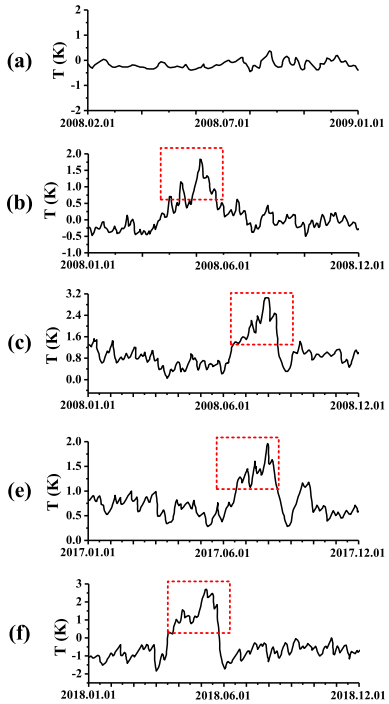

FIGURE 10. Brightness temperature difference one year before and after the earthquake in each area. Note: Fig. (a) shows the brightness temperatures in the area without earthquakes in Sichuan from February 1, 2008, to January 1, 2009. Fig. (b) shows the brightness temperatures between February 1, 2008, and January 1, 2009, in Wenchuan, Sichuan. Fig. (c) shows the brightness temperatures in Zhongba, Tibet from January 1, 2008, to December 1, 2008. Fig. (d) shows the brightness temperatures in the Jinghe River, Xinjiang, from January 1, 2017, to December 1, 2017. Fig. (e) shows the brightness temperatures in Jilin Songyuan from January 1, 2008, to December 1, 2008. The dotted box shows when an earthquake occurs.

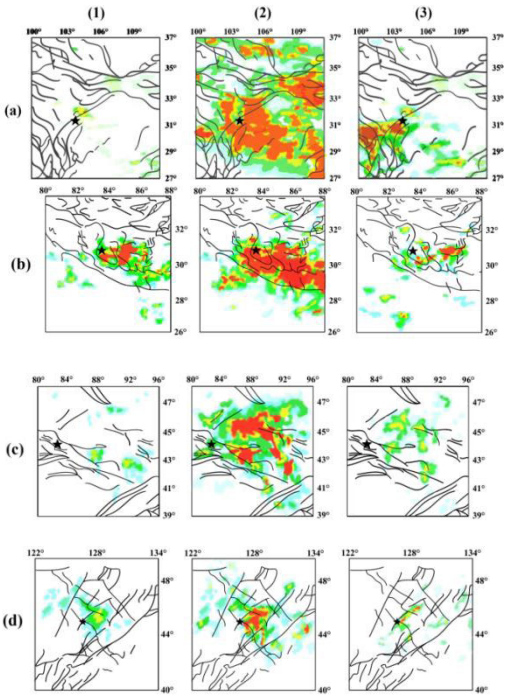

FIGURE 11. Spatiotemporal variation in the relative infrared power spectrum of earthquake middle waves in different regions. Note: Fig. (a) shows the spatiotemporal variation in the relative infrared power spectrum of the mid-wave earthquakes in Wenchuan, Sichuan Province from January 1, 2008, to December 1, 2008. Fig. (b) shows the spatiotemporal variation in the relative infrared power spectrum of the mid-wave earthquakes in Zhongba, Tibet from January 1, 2008, to December 1, 2008. Fig. (c) shows the spatiotemporal variation in the infrared relative power spectrum of the mid-wave earthquake in Jinghe, Xinjiang from January 1, 2017, to December 1, 2017. Fig. (d) shows the spatiotemporal variation in the relative infrared power spectrum of the mid-wave earthquake in Songyuan, Jilin Province, from January 1, 2018, to December 1, 2018. Fig. (1) shows the month before the earthquake. Fig. (2) shows the month of the earthquake; Fig. (3) shows the month after the earthquake. The pentagram shows the epicenter of each earthquake.

this study is designed with several interfaces, including user login information (user name and password input), function selection (optional options include information management, prediction and early warning, command scheduling, and simulation drills), information management (to display satellite remote sensing data in earthquake areas), prediction and early warning (to display the assessment of the number of rescue forces and machinery in different earthquake areas), command and dispatching (to display the tents, drugs, and the reserve of food and drinking water in different areas), and simulation exercises (including adjustment options such as earthquake amplitude, earthquake area, earthquake time to simulate the effect of earthquake zone command and dispatch during earthquakes). The output system interface is shown in Fig. 13.

E. INDEX CONSTRUCTION OF THE EARTHQUAKE EMERGENCY COMMAND SYSTEM BASED ON CLOUD COMPUTING AND IoT

To develop the earthquake emergency command system based on cloud computing and IoT more comprehensive and precise in the evaluation of index construction, the analysis method from multiple angles in which departments involved in earthquake emergency command system is not considered. Thus, we only build the proposed earthquake emergency command system based on new technology from the perspective of the user of the system-earthquake emergency department [34]. Based on the necessity and possibility of earthquake emergency command systems, literature analysis, and expert consultation results, an evaluation system for the earthquake emergency command system is constructed in this study, including 5 first indices and 15 second indices, as shown in Fig. 14. The description of the function of each index is shown in Fig. 14.

The weight of the index is the importance and contribution of the various indices in a system for the system [35]. There are many computing methods of weight, and AHP is used in the study, which breaks down the index to the levels of goal, criteria and solution and conducts quantitative or qualitative analysis [36].

The AHP includes four steps. First, the problems that require decision making are broken down based on different goals or criteria, and the earthquake emergency command system can be divided into four different layers (target layer,

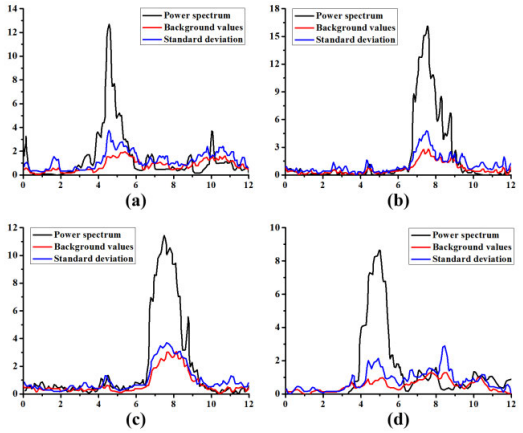

FIGURE 12. Time series of the relative middle wave infrared power spectrum in each region within one year. Note: Fig. (a) shows the time series of the relative infrared power spectrum of the mid-wave earthquakes in Wenchuan, Sichuan Province, from January 1, 2008, to December 1, 2008. Fig. (b) shows the time series of the relative infrared power spectrum of the mid-wave earthquakes in Zhongba, Tibet from January 1, 2008, to December 1, 2008. Fig. (c) shows the time series of the relative infrared power spectrum of the earthquake middle wave from January 1, 2017, to December 1, 2017, in Jinghe, Xinjiang. Fig. (d) shows the time series of the relative infrared power spectrum of the mid-wave earthquakes in Songyuan, Jilin Province from January 1, 2011, to December 1, 2011.

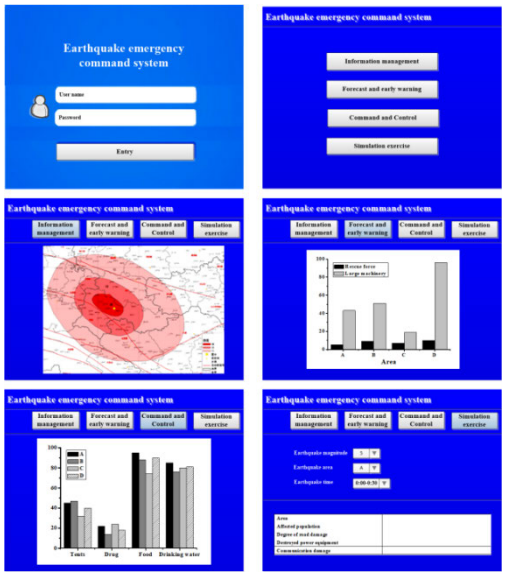

FIGURE 13. Display of the output interface of the earthquake emergency command system.

criteria layer, index layer, and solution layer) based on the study. Second, the judgment matrix must be built, and the judgment matrix compares and judges the importance of evaluation based on the evaluation index. Third, the maximum eigenvalue of the judgment matrix is calculated. Lastly, a consistency check is conducted to the judgment matrix [37], and the equation of the consistency check is:

$$CI = \frac{\lambda_{\max}(A) - n}{n - 1} \tag{16}$$

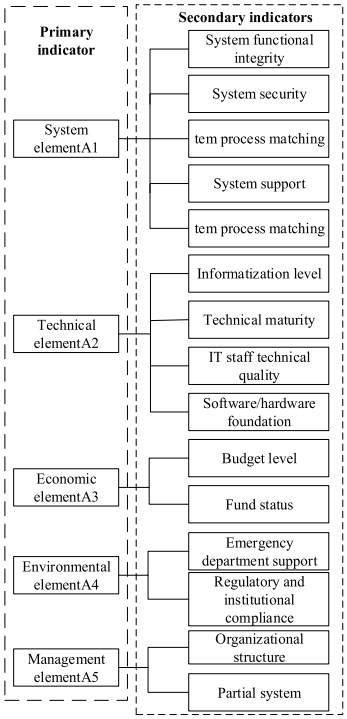

FIGURE 14. First indices and second indices of the system.

The calculation method for the average random consistency index (RI) is as follows. For a fixed n, a comparison matrix A is randomly constructed, and a_{ij} is randomly extracted from 1, 2, . . ., 9, 1/2, 1/3 . . ., 1/9. If A is inconsistent, a sufficiently large A is taken to obtain an average of the maximum eigenvalues of matrix A.

RI is compared to a comparison matrix and describes the average random consistency index; only n can be used as an effective impact index [38]. The calculation method of the consistency ratio is shown in equation (17):

$$CR = CI \big/ RI \tag{17}$$

The consistency ratio (CR) is used to judge the effectiveness of the proposed method. When CR < 0.1, the system is consistent with the comparison matrix (i.e., the result is acceptable). When CR > 0.1, the system is not consistent with the comparison matrix (i.e., the system is not acceptable); the judgment matrix must then be adjusted until consistency is met [39]. The contrast scale table is shown in Table 4.

When the weight of the rating system index is confirmed, it is necessary to calculate the eigenvector W and the maximum eigenvalue $\lambda_{\max}$ of each questionnaire with the summation method. Additionally, the first step of the calculation procedure is normalization processing the vectors in each column of a comparison matrix [40]:

$$B = (b_{i,j}), b_{i,j} = \frac{a_{i,j}}{\sum_{i=1}^{n} a_{i,j}}, \quad i, j = 1, 2, 3, \cdots, n \tag{18}$$

TABLE 2. Description of system evaluation index.

First class index	Second index index	Index description
System elements	System functional integrity a11	Whether the business functions designed in the system meet the requirement of emergency command
	System security a12	Whether the system design agrees with safety standard system
	System process matching degree a13	Matching degree of emergency process designed in the system and that in earthquake emergency department
	System support a14	Support of the system for the realization of earthquake command target
	System sharing a15	Extent of the system for realizing the sharing of software and hardware
Technical elements	Informationalized level a21	Informationalized level of earthquake emergency department
	Technical maturity a22	Maturity of the new generation of technology in the application of emergency field
	Technical quality of IT personnel a23	Technical level of IT personnel in earthquake emergency department
	Software/hardware basis a24	Basic level of software and hardware of earthquake emergency department
Economic level	Budget level a31	The level of budget available to the emergency department for system construction
	Finial status a32	Current funding status of the emergency department
Environmental elements	Emergency department support a41	Support degree of emergency department for system development
	Compliance with laws and regulations a42	Whether it conforms to the current state of the law, regulations
Management elements	Organizational structure a51	Standardization of organizational structure of emergency department
	Division system a52	The perfection of the system of earthquake emergency department

TABLE 3. Modified value comparison table of consistency check.

N	1	2	3	4	5	6	7	8	9
RI	0	0	0.56	0.91	1.11	1.23	1.31	1.40	1.44

TABLE 4. Contrast scale table.

Scale value	Comparison standard (index ai, aj)
1	Both indexes are equally important
2	Between the upper and lower criteria
3	Index ai is more important
4	Between the upper and lower criteria
5	Index ai is very important
6	Between two criteria
7	Index ai is very important
8	Between two criteria
9	Index ai is extremely important

Then, we sum each line of $B = (b_{i,j})$, and the following equations are obtained:

$$C = (\mathrm{C}_1, \mathrm{C}_2, \mathrm{C}_3, \cdots, \mathrm{C}_n)^T \tag{19}$$

$$C_i = \sum_{i=1}^{n} b_{i,j}, \quad i, j = 1, 2, 3, \cdots, n \tag{20}$$

Next, we normalize C, and the following equation is obtained:

$$W = (\mathrm{W}_1, \mathrm{W}_2, \mathrm{W}_3, \cdots, \mathrm{W}_N)^T \tag{21}$$

$$W_i = C_i \Big/ \sum_{i=1}^{n} C, \quad i, j = 1, 2, 3, \cdots, n \tag{22}$$

Finally, the maximum eigenvalue is calculated through equation (8):

$$\lambda_{\max} = 1 \Big/ (n(\sum_{i=1}^{n} AW_i / W_i)) \tag{23}$$

where (AW_i) is the i^{th} component of AW.

The average weights of the first-class indices are calculated based on these procedures, as shown in Table 4. When the weight of the feasibility evaluation index is confirmed, 20 persons from the earthquake emergency department are selected to evaluate the importance of each index. A comparison matrix is built based on the evaluation of 20 persons; computing and consistency checks are performed based on the procedures of AHP; and the weights that pass the consistency check are acceptable [41]. Finally, the arithmetic mean is calculated for the weights of various indices, as shown in Table 5. Table 6 shows the weights of the evaluation system

TABLE 5. Evaluation weights of first class indexes.

Index	A	B	C	D	E	F	G	H	I	Average value
A1	0.48	0.45	0.57	0.51	0.46	0.55	0.56	0.53	0.50	0.51
A2	0.10	0.09	0.09	0.12	0.13	0.19	0.17	0.17	0.15	0.16
A3	0.22	0.22	0.13	0.14	0.19	0.10	0.06	0.18	0.11	0.15
A4	0.11	0.13	0.12	0.10	0.14	0.08	0.09	0.06	0.12	0.10
A5	0.09	0.12	0.09	0.13	0.08	0.08	0.12	0.06	0.12	0.08

of the earthquake emergency command system and highlights that earthquake emergency personnel focus on index AI in the first class indices. Personnel tend to focus on a11 primarily in the first class index (system functional integrity) and tend to ignore indices A4 and A5. They also tend to ignore a13 in the second class indexes (system process matching)

F. EVALUATION RESULT OF IMPLEMENTATION FEASIBILITY OF THE EARTHQUAKE EMERGENCY COMMAND SYSTEM BASED ON CLOUD COMPUTING AND IoT

When the implementation feasibility of the earthquake emergency command system is evaluated based on cloud computing and IoT, 20 experts from earthquake emergency departments are chosen to test various indices, and results are shown in Table 7.

The evaluation grade set V = (7,5,3,1), wherein the items represent excellent, better, good and poor evaluation grades, respectively, and comprehensive grade evaluation of second indices can be represented with equation (9):

$$\begin{aligned} B_1 &= A_1^* R_1 \\ &= (0.30, 0.23, 0.09, 0.21, 0.17) \\ &\quad * \begin{pmatrix} 0.55 & 0.25 & 0.20 & 0.00 \\ 0.60 & 0.15 & 0.16 & 0.10 \\ 0.45 & 0.30 & 0.20 & 0.05 \\ 0.50 & 0.29 & 0.10 & 0.10 \end{pmatrix} \\ &= (0.52, 0.22, 0.17, 0.09) \end{aligned} \tag{24}$$

Table 2 shows that 51.9% of respondents think that the earthquake emergency command system yields good results,

TABLE 6. Weights of the evaluation system index of the earthquake emergency command system.

First class index	Weight	Second class index	Weight
System element A1	0.50	System function integrity a11	0.29
		System security a12	0.32
		System process matching degree a13	0.08
		System support a14	0.21
		System sharing a15	0.17
Technical element A2	0.17	Informationalization level a21	0.26
		Technical maturity a22	0.37
		Quality of IT personnel a23	0.28
		Software/hardware basis a24	0.12
Economic element A3	0.14	Budget level a31	0.68
		Financial status a32	0.32
Environmental element A4	0.09	Emergency department support a41	0.65
		Conformity of laws and regulations a42	0.35
Management element A5	0.07	Organizational structure a51	0.70
		Division system a52	0.30

8.1% think that results are poor, and 41% of respondents are undecided. These results change a value within equation (25):

$$F_1 = B_1^* V^T = (0.52, 0.22, 0.17, 0.09)^*(7, 5, 3, 1)^T = 5.43 \tag{25}$$

Ditto,

$$B_2 = (0.71, 0.12, 0.08, 0.09), \quad F_2 = 5.7 \tag{26}$$

$$B_3 = (0.51, 0.17, 0.13, 0.11), \quad F_3 = 5.3 \tag{27}$$

$$B_4 = (0.65, 0.11, 0.09, 0.11), \quad F_4 = 5.53 \tag{28}$$

$$B_5 = (0.42, 0.21, 0.17, 0.21), \quad F_5 = 4.2 \tag{29}$$

$$\begin{aligned} B &= A^* R \\ &= (0.50, 0.17, 0.15, 0.11, 0.08) \\ &\quad * \begin{pmatrix} 0.55 & 0.25 & 0.20 & 0.00 \\ 0.69 & 0.15 & 0.16 & 0.10 \\ 0.48 & 0.30 & 0.20 & 0.05 \\ 0.53 & 0.29 & 0.10 & 0.10 \end{pmatrix} \\ &= (0.55, 0.22, 0.14, 0.11) \end{aligned} \tag{30}$$

TABLE 7. Test results of the first class indices and second indices of the system.

First class index	Second class index	A	B	C	D
System element A1	System function integrity a11	11	4	3	0
	System security a12	12	2	2	2
	System process matching degree a13	10	5	3	1
	System support a14	14	4	3	3
	System sharing a15	15	3	1	5
Technical element A2	Information alization level a21	13	2	1	1
	Technical maturity a22	15	1	1	1
	Quality of IT personnel a23	11	1	1	4
	Software/hardware basis a24	12	2	1	1
Economic element A3	Budget level a31	8	6	1	2
	Financial status a32	12	3	2	1
Environmental element A4	Emergency department support a41	16	1	4	3
	Conformity of laws and regulations a42	16	1	1	1
Management element A5	Organizational structure a51	16	3	5	3
	Division system a52	8	5	2	3

Note: A, B, C and D represent excellent, better, good and poor evaluation grades, respectively.

Finally, the score obtained is 5.36, and the total score of the earthquake emergency command system is higher than that in the better grade; thus, the system can provide good results.

V. CONCLUSION

This study aims to solve various problems in earthquake rescue. Cloud computing and IoT are used in the design of the proposed earthquake emergency command system. First, the characteristics of surface radiation, brightness temperature difference, and relative power spectrum before and after earthquakes in China in recent years are analyzed based on satellite infrared remote sensing data. Data before the earthquake is found to provide the basis for the accurate prediction of earthquakes. Then, an earthquake emergency system that uses cloud computing and IoT is constructed and tested with satellite infrared remote sensing data. AHP is used in the system from the perspective of the earthquake emergency department, and we show that the system yields a better grade score based on a fuzzy rating scale regardless of the elements of technology, economy and system; thus, the proposed system yields good results.

Although this study demonstrates an alternative pathway to develop earthquake command systems, earthquakes are complex, and there are various challenges in earthquake rescue. There may be limitations in the realization of the functions proposed in this system, and better system functions must be developed.

REFERENCES

[1] L. Qin, S. Feng, and H. Zhu, "Research on the technological architectural design of geological hazard monitoring and rescue-after-disaster system based on cloud computing and Internet of Things," *Int. J. Syst. Assurance Eng. Manage.*, vol. 9, no. 3, pp. 684–695, Jun. 2018, doi: 10.1007/s13198-017-0638-0.

[2] T. Bhatia and A. K. Verma, "Data security in mobile cloud computing paradigm: A survey, taxonomy and open research issues," *J. Supercomput.*, vol. 73, no. 6, pp. 2558–2631, Jan. 2017, doi: 10.1007/s11227-016-1945-y.

[3] C. Mouradian, N. T. Jahromi, and R. H. Glitho, "NFV and SDN-based distributed IoT gateway for large-scale disaster management," *IEEE Internet Things J.*, vol. 5, no. 5, pp. 4119–4131, Oct. 2018, doi: 10.1109/JIOT.2018.2867255.

[4] H. Ning, X. Liu, X. Ye, J. He, W. Zhang, and M. Daneshmand, "Edge computing-based ID and nID combined identification and resolution scheme in IoT," *IEEE Internet Things J.*, vol. 6, no. 4, pp. 6811–6821, Aug. 2019, doi: 10.1109/JIOT.2019.2911564.

[5] N. Ahmad, A. Barkat, A. Ali, M. Sultan, K. Rasul, Z. Iqbal, and T. Iqbal, "Investigation of spatio-temporal satellite thermal IR anomalies associated with the Awaran earthquake (Sep 24, 2013; m 7.7), Pakistan," *Pure Appl. Geophys.*, vol. 176, no. 8, pp. 3533–3544, Mar. 2019, doi: 10.1007/s00024-019-02149-9.

[6] T. J. Wu, "Model design and structure research for integration system of energy, information and transportation networks based on ANP-fuzzy comprehensive evaluation," *Global Energy Interconnection*, vol. 1, no. 2, pp. 137–144, Apr. 2018, doi: CNKI:SUN:ZNDW.0.2018-02-007.

[7] N. Chen, W. Liu, R. Bai, and A. Chen, "Application of computational intelligence technologies in emergency management: A literature review," *Artif. Intell. Rev.*, vol. 52, no. 3, pp. 2131–2168, Oct. 2019, doi: 10.1007/s10462-017-9589-8.

[8] C. K. M. Lee, Y. Lv, K. K. H. Ng, W. Ho, and K. L. Choy, "Design and application of Internet of Things-based warehouse management system for smart logistics," *Int. J. Prod. Res.*, vol. 56, no. 8, pp. 2753–2768, Apr. 2018, doi: 10.1080/00207543.2017.1394592.

[9] Z. H. Lv, X. M. Li, and K. K. R. Choo, "E-government multimedia big data platform for disaster management," *Multimedia Tools. Appl.*, vol. 77, no. 8, pp. 10069–10077, 2018, doi: 10.1007/s11042-017-5119-6.

[10] H. Vasyura-Bathke, J. Dettmer, A. Steinberg, S. Heimann, M. P. Isken, O. Zielke, P. M. Mai, H. Sudhaus, and S. Jónsson, "The Bayesian earthquake analysis tool," *Seismol. Res. Lett.*, vol. 91, no. 2, pp. 1003–1018, Jan. 2020, doi: 10.1785/0220190075.

[11] T. Murota and F. Takeda, "A discussion on the nation's command and coordination regarding emergency fire response teams," *J. Disaster Res.*, vol. 14, no. 7, pp. 978–990, 2019, doi: 10.20965/jdr.2019.p0978.

[12] A. J. Imperiale and F. Vanclay, "Command-and-control, emergency powers, and the failure to observe united nations disaster management principles following the 2009 L'Aquila earthquake," *Int. J. Disaster Risk Reduction*, vol. 36, May 2019, Art. no. 101099, doi: 10.1016/j.ijdrr.2019.101099.

[13] T. Wang, S. Guomai, L. Zhang, G. Li, Y. Li, and J. Chen, "Earthquake emergency response framework on campus based on multi-source data monitoring," *J. Cleaner Prod.*, vol. 238, Nov. 2019, Art. no. 117965, doi: 10.1016/j.jclepro.2019.117965.

[14] J. Xu, H. Zhou, G. Nie, and J. An, "Plotting earthquake emergency maps based on audience theory," *Int. J. Disaster Risk Reduction*, vol. 47, Aug. 2020, Art. no. 101554, doi: 10.1016/j.ijdrr.2020.101554.

[15] F. Ahmadzadeh, N. Mohammadi, and M. Babaie, "Evaluation the emergency response program of emergency operations command center of the Alborz University of medical sciences in response to Kermanshah earthquake in Nov. 2017," *Health Emergencies Disasters*, vol. 4, no. 3, pp. 135–146, 2019, doi: 10.3390/rs12010062.

[16] X. Yao, G. Li, J. Xia, J. Ben, Q. Cao, L. Zhao, Y. Ma, L. Zhang, and D. Zhu, "Enabling the big Earth observation data via cloud computing and DGGS: Opportunities and challenges," *Remote Sens.*, vol. 12, no. 1, p. 62, Dec. 2019, doi: 10.3390/rs12010062.

[17] P. Arroyo, J. Herrero, J. Suárez, and J. Lozano, "Wireless sensor network combined with cloud computing for air quality monitoring," *Sensors*, vol. 19, no. 3, p. 691, Feb. 2019, doi: 10.3390/s19030691.

[18] E. C. d'Oro, S. Colombo, M. Gribaudo, M. Iacono, D. Manca, and P. Piazzolla, "Modeling and evaluating a complex edge computing based systems: An emergency management support system case study," *Internet Things*, vol. 6, Jun. 2019, Art. no. 100054, doi: 10.1016/j.iot.2019.100054.

[19] D. Facchinetti, G. Psaila, and P. Scandurra, "Mobile cloud computing for indoor emergency response: The IPSOS assistant case study," *J. Reliable Intell. Environ.*, vol. 5, no. 3, pp. 173–191, Jul. 2019, doi: 10.1007/s40860-019-00088-9.

[20] K. C. Ujjwal, S. Garg, J. Hilton, J. Aryal, and N. Forbes-Smith, "Cloud computing in natural hazard modeling systems: Current research trends and future directions," *Int. J. Disaster Risk Reduction*, vol. 38, Aug. 2019, Art. no. 101188, doi: 10.1016/j.ijdrr.2019.101188.

[21] L. Liu, C.-F. Li, X.-K. Sun, and J.-J. Zhao, "Event alert and detection in smart cities using anomaly information from remote sensing earthquake data," *Comput. Commun.*, vol. 153, pp. 397–405, Mar. 2020, doi: 10.1016/j.comcom.2020.02.023.

[22] A. Barkat, A. Ali, K. Rehman, M. Awais, M. S. Riaz, and T. Iqbal, "Thermal IR satellite data application for earthquake research in Pakistan," *J. Geodynamics*, vol. 116, pp. 13–22, May 2018, doi: 10.1016/j.jog.2018.01.008.

[23] C. Wei, X. Lu, Y. Zhang, Y. Guo, and Y. Wang, "A time-frequency analysis of the thermal radiation background anomalies caused by large earthquakes: A case study of the Wenchuan 8.0 earthquake," *Adv. Space Res.*, vol. 65, no. 1, pp. 435–445, Jan. 2020, doi: 10.1016/j.asr.2019.09.019.

[24] F. Jing, R. P. Singh, Y. Cui, and K. Sun, "Microwave brightness temperature characteristics of three strong earthquakes in Sichuan province, China," *IEEE J. Sel. Topics Appl. Earth Observ. Remote Sens.*, vol. 13, pp. 513–522, 2020, doi: 10.1109/JSTARS.2020.2968568.

[25] Y.-P.-E. Wang, X. Lin, A. Adhikary, A. Grovlen, Y. Sui, Y. Blankenship, J. Bergman, and H. S. Razaghi, "A primer on 3GPP narrowband Internet of Things," *IEEE Commun. Mag.*, vol. 55, no. 3, pp. 117–123, Mar. 2017, doi: 10.1109/MCOM.2017.1600510CM.

[26] L. Dong, W. Shu, D. Sun, X. Li, and L. Zhang, "Pre-alarm system based on real-time monitoring and numerical simulation using Internet of Things and cloud computing for tailings dam in mines," *IEEE Access*, vol. 5, pp. 21080–21089, 2017, doi: 10.1109/ACCESS.2017.2753379.

[27] S. Liu, L. Guo, H. Webb, X. Ya, and X. Chang, "Internet of Things monitoring system of modern eco-agriculture based on cloud computing," *IEEE Access*, vol. 7, pp. 37050–37058, 2019, doi: 10.1109/ACCESS.2019.2903720.

[28] Z. Liu, "Research on the Internet of Things and the development of smart city industry based on big data," *Cluster Comput.*, vol. 21, no. 1, pp. 789–795, Mar. 2018, doi: 10.1007/s10586-017-0910-8.

[29] F. Riaz and M. A. Niazi, "Road collisions avoidance using vehicular cyber-physical systems: A taxonomy and review," *Complex Adapt. Syst. Model.*, vol. 4, no. 1, p. 15, Jul. 2016, doi: 10.1186/s40294-016-0025-8.

[30] C. H. Chi, "Examining the disaster response twenty years after the 1999 Chi-Chi Earthquake," *J. Acute Med.*, vol. 9, no. 3, pp. 81–82, 2019, doi: 10.6705/j.jacme.201909_9(3).0001.

[31] J. D. C. Silva, A. B. D. O. Dantas, and F. H. D. Carvalho, "A scientific workflow management system for orchestration of parallel components in a cloud of large-scale parallel processing services," *Sci. Comput. Program.*, vol. 173, pp. 95–127, Mar. 2019, doi: 10.1016/j.scico.2018.04.004.

[32] J. Haussmann, W. Blochinger, and W. Kuechlin, "Cost-efficient parallel processing of irregularly structured problems in cloud computing environments," *Cluster Comput.*, vol. 22, no. 3, pp. 887–909, Sep. 2019, doi: 10.1007/s10586-018-2879-3.

[33] W. Chen, H. Zhang, L. K. Comfort, and Z. Tao, "Exploring complex adaptive networks in the aftermath of the 2008 Wenchuan earthquake in China," *Saf. Sci.*, vol. 125, May 2020, Art. no. 104607, doi: 10.1016/j.ssci.2020.104607.

[34] C. Heskey, K. Oda, and J. Sabaté, "Avocado intake, and longitudinal weight and body mass index changes in an adult cohort," *Nutrients*, vol. 11, no. 3, p. 691, Mar. 2019, doi: 10.3390/nu11030691.

[35] P. H. Dos Santos, S. M. Neves, D. O. Sant'Anna, C. H. D. Oliveira, and H. D. Carvalho, "The analytic hierarchy process supporting decision making for sustainable development: An overview of applications," *J. Cleaner Prod.*, vol. 212, pp. 119–138, Mar. 2019, doi: 10.1016/j.jclepro.2018.11.270.

[36] H. K. Chan, X. Sun, and S.-H. Chung, "When should fuzzy analytic hierarchy process be used instead of analytic hierarchy process?" *Decis. Support Syst.*, vol. 125, Oct. 2019, Art. no. 113114, doi: 10.1016/j.dss.2019.113114.

[37] Z. Shi, Y. Ouyang, R. Qiu, S. Hu, Y. Zhang, M. Chen, and P. Wang, "Bioinspired superhydrophobic and oil-infused nanostructured surface for Cu corrosion inhibition: A comparison study," *Prog. Organic Coat.*, vol. 131, pp. 49–59, Jun. 2019, doi: 10.1016/j.porgcoat.2019.02.004.

[38] X. Mi, M. Tang, H. Liao, W. Shen, and B. Lev, "The state-of-the-art survey on integrations and applications of the best worst method in decision making: Why, what, what for and what's next?" *Omega*, vol. 87, pp. 205–225, Sep. 2019, doi: 10.1016/j.omega.2019.01.009.

[39] S. A. Ali and A. Ahmad, "Mapping of mosquito-borne diseases in Kolkata municipal corporation using GIS and AHP based decision making approach," *Spatial Inf. Res.*, vol. 27, no. 3, pp. 351–372, Jan. 2019, doi: 10.1007/s41324-019-00242-8.

[40] H. Sattar, "Effect of parameter setting and spectral normalization approach on study of matrix effect by laser induced breakdown spectroscopy of Ag-Zn binary composites," *Plasma Sci. Technol.*, vol. 21, no. 3, Jan. 2019, Art. no. 034019, doi: CNKI:SUN:DNZK.0.2019-03-021.

[41] D. Bindi, S.-R. Kotha, G. Weatherill, G. Lanzano, L. Luzi, and F. Cotton, "The pan-European engineering strong motion (ESM) flatfile: Consistency check via residual analysis," *Bull. Earthq. Eng.*, vol. 17, no. 2, pp. 583–602, Feb. 2019, doi: 10.1007/s10518-018-0466-x.